AN INVESTIGATION OF THE PRINCIPLES AND TECHNIQUES OF BRAGG DIFFRACTION LASER BEAM PROBING OF AN ULTRASONIC FIELD

Robert David Brown

NAVAL POSTGRADUATE SCHOOL

Monterey, California

THESIS

An Investigation of the Principles and Techniques of Bragg Diffraction Laser Beam Probing of an Ultrasonic Field

by

Robert David Brown, Jr.

Thesis Advisor: John P. Powers

Approved for public release; distribution unlimited.

An Investigation of the Principles and Techniques of Bragg Diffraction Laser Beam Probing of an Ultrasonic Field

by

Robert David Brown, Jr.
Lieutenant, United States Navy
B.S. United States Naval Academy, 1965

Submitted in partial fulfillment of the
requirements for the degree of

MASTER OF SCIENCE IN ENGINEERING ACOUSTICS

from the

NAVAL POSTGRADUATE SCHOOL
December 1972

ABSTRACT

Probing of the near field of an ultrasonic beam in water with a thin laser beam has verified that a diffracted beam of light, whose amplitude is a function of the angle of incident light, is related to the spatial Fourier spectrum of the far-field acoustic distribution. There are indications that this method of probing may be useful in evaluating transducer mountings.

As an application of the technique, reflection-transmission properties of sound on a liquid-liquid interface are examined, and the detection of evanescent waves verifies their physical existence and properties.

TABLE OF CONTENTS

I. INTRODUCTION 4

II. THEORY 7

III. EXPERIMENT 16

IV. APPLICATION 22

V. CONCLUSION 34

BIBLIOGRAPHY 35

INITIAL DISTRIBUTION LIST 36

FORM DD 1473 37

I. INTRODUCTION

The amplitude and phase of an ultrasonic field may be measured with a number of methods in the state of the art.

The most well-known method of obtaining such information is by use of a mechanical piezoelectric probe, such as a hydrophone, inserted into the field, where the pressure fluctuations generate a proportional voltage from which amplitude and phase information at a specific point may be obtained. The Whittaker-Shannon sampling theorem has shown that the acoustic distribution can be completely described when sampled at spatial separations less than $\frac{\Lambda}{2}$ · [1]. For sampling with a single hydrophone, this requires some form of scanning system, and in the sampling process, the time dependence is lost. The time dependence may be preserved by sampling with an array of properly positioned sensors, but the field to be described is limited to the size of the array, and the number of sensing elements needed is increased as the number of sample points desired increases.

A further disadvantage of this technique exists specifically at frequencies in the megahertz range. The physical size of the sampling device must be much less than $\frac{\Lambda}{2}$ to avoid perturbing the sound field and to resolve features of the field. The large number of such devices necessary for an array of large size and the attendant cost associated with miniaturization soon becomes prohibitive, and practically speaking, array sampling is presently limited to frequencies not much above one megahertz.

The advent of the laser has made practical alternative methods of probing a sound field particularly suited to the megahertz region and above. One of these methods, utilizing the principle of Bragg diffraction, involves a focused laser beam to probe a sound field [2], and can provide real-time amplitude and phase information in three dimensions. By making use of certain polarization effects or by spatially filtering the diffracted light, a photodiode may be used to capture complex pressure information in a limited zone about the optical beam focus. Within its operational parameters this system offers the most information for the effort required. Scanning the sound field in a volume with this arrangement is difficult, however. Any mechanical scanning system such as moving the sound field along the optic axis to scan its depth (width) requires a highly planar system to preserve phase information.

An alternative to this procedure is to vary the focal length of the lens such that the focused spot scans across the sound field. The difficulty with this is that increasing the focal length increases the diameter of the focused spot. Since the minimum number of wave lengths of sound which can be resolved is proportional to the diameter of the focused spot, resolution decreases with depth.

A third method (to be investigated in this work) also employs the principle of Bragg diffraction, and is the probing of the sound field with a thin "pencil" beam of light. The incident light interacts with the sound to produce a diffracted ray of light to which acoustic amplitude and phase information has been transferred. The frequency of this diffracted ray of light is doppler-shifted by an amount equal to the frequency of the sound. The intensity of the diffracted light, as a function of the angle of the probing beam, is directly related to the intensity of the spatial Fourier spectrum of the ultrasonic field.[3]

While this method is constrained to optically transparent liquids and solids, amplitude information of the sound field can be easily obtained by direct detection, and phase information can be extracted by mixing the diffracted and undiffracted light to obtain a difference frequency. The real advantage of the pencil beam probe, however, lies in the inherent simplicity with which amplitude information in one dimension may be obtained.

The technique of probing with such a thin pencil of light in a liquid medium is presented here for an acoustic field with slits of different widths. The application of this approach in examining acoustical critical angle phenomena at a liquid-liquid interface is also demonstrated. Specifically, this method is used to detect the presence of the evanescent waves generated by an acoustical signal impinging on a liquid-liquid interface at angles greater than or equal to the critical angle of incidence, as well as the incident and reflected beams at the interface. Simple measurements confirm the expected properties of the evanescent waves, verifying their existence.

II. THEORY

When light interacts with an ultrasonic field, diffracted light components can be generated at frequencies equal to the sum or difference of the light frequency and harmonics of the sound frequency. [3,4] This can be described qualitatively [5] by considering that any given portion of the sonic medium expands and contracts periodically under the influence of a periodic pressure wave, resulting in simultaneous changes in the optical index of refraction for the medium in that particular region at that particular time.

When coherent light is normally incident on the sound field, a "gradation" of diffracted light components occurs, the amount of which is related to the degree of compression or rarefaction in the medium. Destructive interference effects over the width of the sound field, however, result in cancellation of part of the diffracted components. For narrow sound fields this has the effect that the diffracted components which survive are the first, second, third-order sidebands, etc. Interactions of this nature are said to occur in the "Debye-Sears" or "Raman-Nath" regime.

Beyond a critical width of the sound field, additional interference takes place which successfully cancels all of the diffracted light. However, by reorienting the incident light, the interference effects can be worked to reinforce the diffracted components so that the construction of one particular sideband is possible. This occurs when the field width satisfies $\frac{K^2L}{k} > \pi$, where K and k are the propagation constants of the sound and incident light respectively, and L is the width of the sound

field. The angle of reorientation away from the normal required for growth of the first order sideband is the Bragg angle, given by

$$\sin \theta_B = \frac{\lambda}{2\Lambda} \qquad (2.1)$$

where λ and Λ are the wavelengths of the light and sound respectively.

The first upper sideband (i.e., the sideband with increased frequency) results if the incident light is directed into the advancing sound as shown in Fig. (1a) while the first lower sideband (i.e., the one with decreased frequency) results from the incident light being directed away from the advancing sound as in Fig. (1b). Similarly, interaction at twice the Bragg angle yields the second-order sideband (with frequencies shifted by twice the sound frequency) exclusively, and so on for higher angles. Additionally, the amplitude of each successive order sideband is diminished. For what follows, however, only the first-order interaction will be addressed.

In this interaction first-order upper and lower sideband generation can be viewed as parametric ampliciation in travelling waves. [6,5] Thus

$$\omega_{\pm 1} = \omega_i \pm \Omega \qquad (2.2)$$

where $\omega_{\pm 1}$ is the angular frequency of the upshifted or downshifted frequency, ω_i is the angular frequency of the incident light, and Ω is the angular frequency of sound. Figure (1) shows the parametric effect. Since the magnitude of ω_i is on the order of 10^{15} rad/sec and Ω is on the order of 10^7 rad/sec, it should be noted that there is little difference in the angular frequencies of ω_i and $\omega_{\pm 1}$.

The angle of departure of the diffracted light is equal to the angle of incidence, i.e., the Bragg angle. Conceptually, the interaction is easily explained in terms of plane waves: a plane wave of light interacts

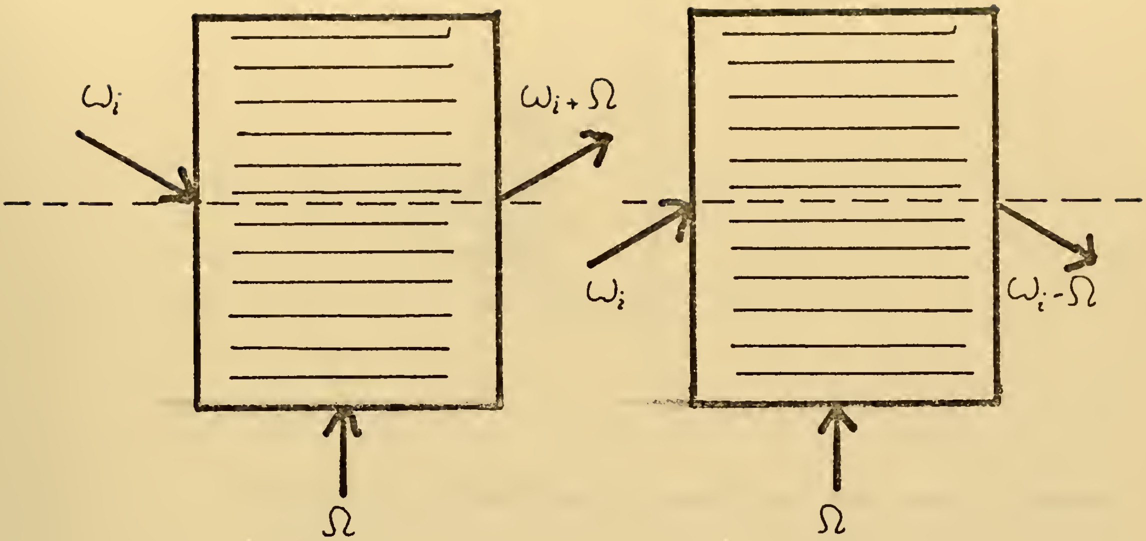

(a) (b)

Figure (1) Generation of (a) upper and (b) lower sideband frequencies during Bragg diffraction

with a plane wave of sound to produce a plane wave of diffracted light. Figure (2) depicts the geometry of the situation. The vectors $\vec{K}$, $\vec{k}$, and $\vec{k}_{\pm 1}$ represent the propagation vectors of plane waves of sound, incident light, and first-order diffracted light respectively. [7]

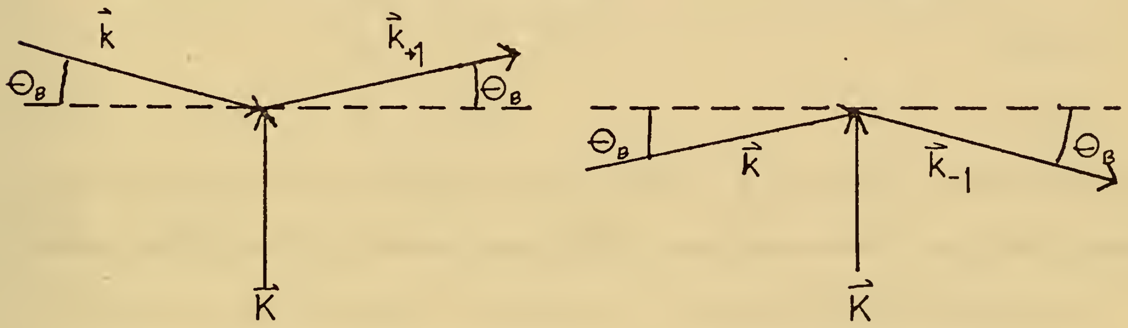

(a) (b)

Figure (2) Geometry for (a) upper sideband generation, (b) lower sideband generation

Because the magnitudes of $\omega_{\pm 1}$ and ω_i are very nearly equal, $|\vec{k}_{\pm 1}| = |\vec{k}|$. Rearranging Fig. (2a) into an isosceles triangle (the "Bragg Triangle" as shown in Fig. (3)), it is possible to determine the Bragg angle:

$$\sin \theta_B = \frac{|\vec{K}/2|}{|\vec{k}|} = \frac{\lambda}{2\Lambda} \qquad (2.3)$$

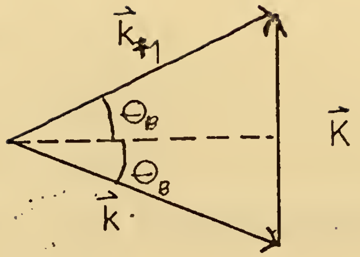

Figure (3) The Bragg Triangle for the upper sideband

The preceding relationships can also be derived from a quantum mechanics point of view by considering the interaction as a photon-phonon interaction. [6] The optical radiation is comprised of photons whose momentum can be written $\hbar\vec{k}$, and energy $hf=\hbar\omega$, where h=Planck's constant. Similarly, the sonic radiation is composed of phonons of momentum $\hbar\vec{K}$ and energy $\hbar\Omega$. Thus, for the conditions stated above,

$$\omega_{\pm1} = \omega_i \pm \Omega \tag{2.4}$$

and

$$\vec{k}_{\pm1} = \vec{k} \pm \vec{K} \tag{2.5}$$

the following interpretation can be made: a photon of energy $\hbar\omega$ and momentum $\hbar\vec{k}$ and a phonon of energy $\hbar\Omega$ and momentum $\hbar\vec{K}$ are both destroyed, creating in the process a new photon of energy $\hbar(\omega_i\pm\Omega)$ and momentum $\hbar(\vec{k}\pm\vec{K})$ such that both energy and momentum are conserved. Equations (2.4) and (2.5) when multiplied by $\hbar$ are then just statements of the conservation of energy and momentum in the collision.

It can be shown [8] that given the requisite orientation for Bragg diffraction, the amplitude of the diffracted light is directly related to the product of the amplitudes of the incident light and sound. Further, the phase of the upshifted version is the sum of the phases of

the incident light and the sound, while the downshifted phase is the difference between the two.

Thus $$|U_{\pm1}| \; \alpha \; |U_l||U_s| \tag{2.6}$$

and $$\phi_{+1} = \phi_l + \phi_s \tag{2.7}$$

$$\phi_{-1} = \phi_l - \phi_s \tag{2.8}$$

which can be combined in the following manner:

$$\underline{U}_{+1} \; \alpha \; \underline{U}_l \; \underline{U}_s \tag{2.9}$$

$$\underline{U}_{-1} \; \alpha \; \underline{U}_l \; \underline{U}_s^{*} \tag{2.10}$$

where $$\underline{U}_{\pm1} = |U_{\pm1}| e^{j\phi_{\pm1}} \tag{2.11}$$

is the standard phasor notation of a quantity having both amplitude and phase, and * denotes complex conjugate.

Since the discussion of the interaction has so far been limited to an interaction between plane waves, it now becomes useful to consider the decomposition of an arbitrary cross section of a complex-valued wave function into an aggregate of plane wave components. [1,7] Let $\underline{U}(x,y,z_o)$ be such a complex-valued wave function travelling in the z direction and located at z_o. This can be described by

$$\underline{U}(x,y,z_o) = \iint_{-\infty}^{\infty} \underline{U}(f_x,f_y,z_o) e^{-j2\pi(f_x x + f_y y)} df_x df_y \tag{2.12}$$

where $e^{-j2\pi(f_x x + f_y y)}$ describes a plane wave with a propagation direction that is specified by

$$f_x = \frac{\alpha}{\lambda} \tag{2.13}$$

$$f_y = \frac{\beta}{\lambda} \tag{2.14}$$

$$f_z = \frac{\gamma}{\lambda} \tag{2.15}$$

where α, β, γ are the direction cosines of the plane wave with respect to the x, y, and z axes respectively, and

$$\gamma = \sqrt{1 - \alpha^2 - \beta^2} \tag{2.16}$$

The function $\underline{U}'\ (f_x,f_y,z_o)$ is simply a weighting function acting on the plane wave amplitude and phase so that when they are assembled over all directions they form the original cross section $\underline{U}\ (x,y,z_o)$. The weighting function $\underline{U}'(f_x,f_y,z_o)$ is defined by

$$\underline{U}'(f_x,f_y,z_o) = \int\!\!\int_{-\infty}^{\infty} \underline{U}(x,y,z_o)\, e^{j2\pi(f_x x+f_y y)}\, dx\, dy \tag{2.17}$$

For the situation specified above, this decomposition takes on the form of the inverse spatial Fourier transform (symbolized by the operator $\mathcal{F}^{-1}\{\ \}$):

$$\underline{U}(x,y,z_o) = \mathcal{F}^{-1}\left\{\underline{U}'(f_x,f_y,z_o)\right\} \tag{2.18}$$

where

$$\underline{U}'(f_x,f_y,z_o) = \mathcal{F}\left\{\underline{U}(x,y,z_o)\right\} \tag{2.19}$$

(Here the operator $\mathcal{F}\{\ \}$ indicates the direct spatial Fourier transform.)

As the function $\underline{U}\ (x,y,z_o)$ is allowed to propagate to a new position z_1, the individual plane wave components $\underline{U}'\ (f_x,f_y)$ also propagate in their respective directions. This may be seen from the following: the complex-valued wave function as a function of z may be described [1] as

$$\underline{U}(x,y,z) = \int\!\!\int_{-\infty}^{\infty} \underline{U}'(f_x,f_y,z_o)\, e^{j2\pi(f_x x+f_y y)}\, e^{j\frac{2\pi z}{\lambda}\sqrt{1-\lambda^2(f_x^2+f_y^2)}}\, df_x\, df_y \tag{2.20}$$

In keeping with the notation of Eq. (1.12), however,

$$\underline{U}(x,y,z_1) = \int\!\!\int_{-\infty}^{\infty} \underline{U}'(f_x,f_y,z_1)\, e^{j2\pi(f_x x+f_y y)}\, df_x\, df_y \tag{2.21}$$

Thus we may conclude

$$\underline{U}'(f_x,f_y,z_1) = \underline{U}'(f_x,f_y,z_o)\, e^{j\frac{2\pi z}{\lambda}\sqrt{1-\lambda^2(f_x^2+f_y^2)}} \tag{2.22}$$

By defining the "transfer function,"

$$\underline{H}(f_x, f_y) = e^{jkz\sqrt{1-\lambda^2(f_x^2+f_y^2)}} \tag{2.23}$$

the total effect of propagation may be written as

$$\underline{U}'(f_x, f_y, z_1) = \underline{H}(f_x f_y)\,\underline{U}'(f_x, f_y, z_0) \tag{2.24}$$

Inspection of Eq. (2.23) reveals that when

$$(\lambda f_x)^2 + (\lambda f_y)^2 < 1 \tag{2.25}$$

propagation over z occurs as a change in relative phase of the plane wave components. When

$$(\lambda f_x)^2 + (\lambda f_y)^2 \geq 1 \tag{2.26}$$

the plane wave is attenuated in the z direction giving rise to evanescent components [1] Evanescent waves will be discussed below.

Having propagated these plane wave components to a new position, z_1, they can now be recombined to form the wave cross section at z_1.

$$\underline{U}(xy, z_1) = \mathcal{F}\left\{\underline{U}'(f_x, f_y, z_1)\right\} \tag{2.27}$$

The advantage to this approach is to be able to treat each of the individual plane wave components separately. Spatial Fourier transformation of the arbitrary light and sound fields into their respective components then allows these individual plane waves of light to interact with the geometrically appropriate plane waves of sound to produce plane waves of diffracted light. The inverse transformation linearly recombines these components into the spatial form of the diffracted light.

For the simplest example of acoustic probing, the entire interaction can be reduced to a single plane of activity by assuming long vertical light and sound sources. The angular spectrum of an infinite vertical line source of light, depicted in Fig. (4), is such that the magnitude

and phase of each component of the spectrum are all equal. The thin pencil of light can be considered to represent any individual plane wave component of that angular spectrum of light. The angular spectrum of sound (shown in Fig. [4]) is that of an infinite vertical slit, where the magnitude and phase are governed by the $\left|\frac{\sin\Theta}{\Theta}\right|$ relationship.

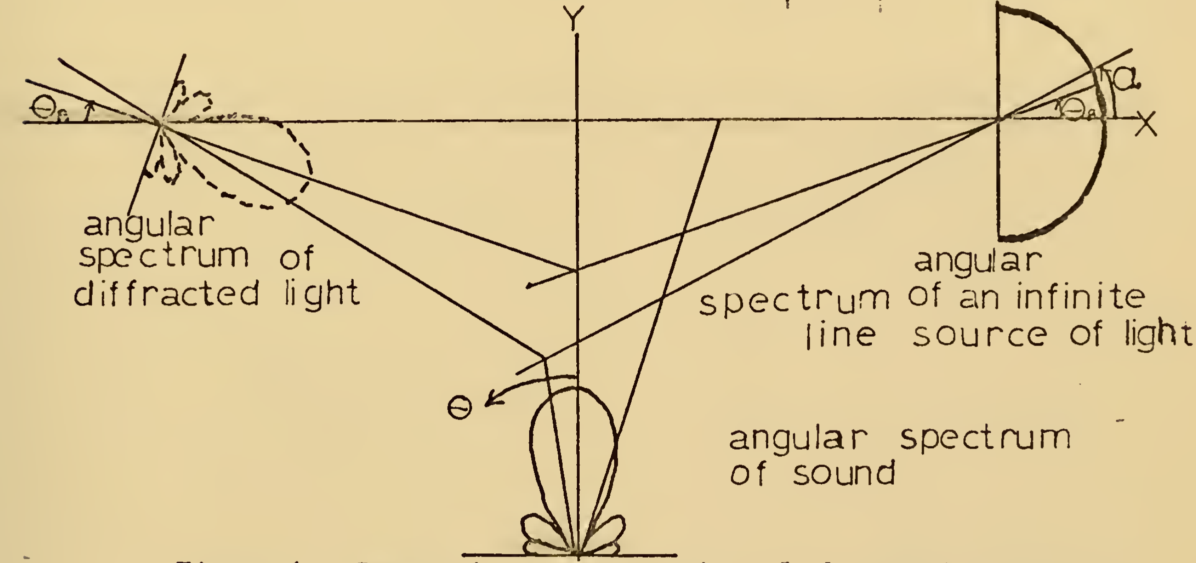

Figure 4. Geometric representation of the angular spectra for downshifted Bragg interaction.

Therefore, when the pencil beam is at an angle Θ_B with respect to the x axis, that plane wave of light is at the geometrically proper angle to interact with the on-axis plane wave component of sound travelling in the y direction. This results in a diffracted component of light proportional in amplitude to the product of the amplitude of the sound component. Similarly, rotation of the laser beam to a new position represents another plane wave component of the infinite line source of light which interacts with its geometrically appropriate plane wave component of sound of a different magnitude. Rotation of the laser beam, then, allows the Bragg interaction to occur over the entire angular spectrum of the sound. With a constant amplitude laser, this has the effect of tracing the magnitude of the angular spectrum of the sound on the

diffracted beam of light. Thus the angular spread of the intensity of the diffracted beam is directly related to the spatial Fourier spectrum of the ultrasonic distribution. [3,8,7]

III. EXPERIMENT

The direct relationship between the amplitude distribution and the angular spread of the spatial Fourier spectrum of the diffracted light was first demonstrated by Cohen and Gordon in 1965 [3] using a thin film cadmium sulfide transducer in a fused quartz medium at frequencies between 50-250 megahertz. For an infinitely long plane wave transducer of width L the amplitude of the diffracted light, as a function of the angle of the incident light is given by

$$\underline{U}'(\alpha) = \underline{b}\,\frac{\sin\left[\frac{1}{2}K(\alpha - \theta_B)L\right]}{\frac{1}{2}K(\alpha - \theta_B)L} \qquad (3.1)$$

where $\underline{U}'$ is the complex amplitude of the diffracted light, α is the angle of rotation with respect to the x axis, $\underline{b}$ is a complex proportionality constant, K is the propagation constant of the sound, and θ_B is the Bragg angle.

In the present situation, a similar experiment was performed using distilled water as the transmission medium at a frequency of 15 megahertz to gain familiarity with the technique. The transducer was gold-plated x-cut quartz operating in the thickness mode with a fundamental frequency of 5 megahertz. The active face of the transducer was 42.5 mm by 42.5 mm. It was mounted with an air backing in an acoustic cell by clamping at the edges. Light from a .3 milliwatt helium neon laser (λ = 6328 Å) was used to probe the sound field through glass windows at a distance of 80-100 mm from the source. A polyethylene acoustic window was located between the source and the light to reduce acoustic swirling. (The noise

added to the diffracted light due to swirling can be significant.) Figure (5) depicts the experimental configuration.

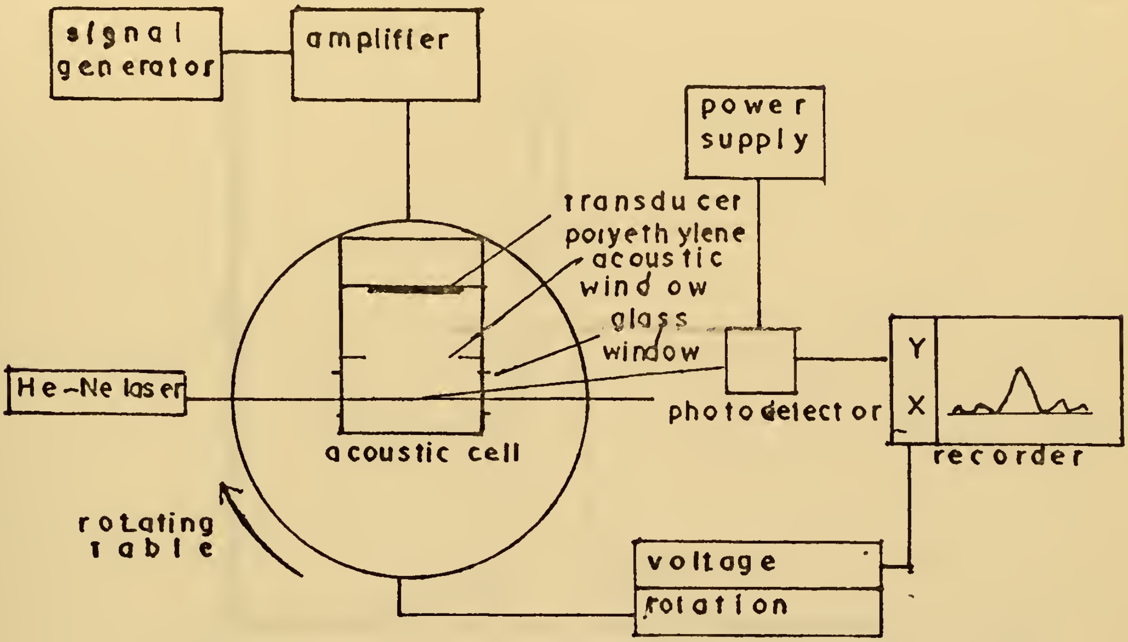

Figure (5) Experimental configuration used in depicting intensity as a function of angle

The acoustic cell was mounted on a mechanical table where table rotation generated a voltage leading to the x axis of the X-Y recorder. The diffracted light was detected by a photodiode, and the resulting signal sent to the y axis. Rotation of the table, then, allowed diffracted light intensity to be recorded as a function of angle. Since rotation of the table with a fixed laser beam versus rotation of the laser with a fixed table involves only a shift of reference, this approach is consistent with the theory presented. Because of the index of refraction of the water-glass-air interface, the angle measured due to table rotation is larger than the angle in the water by a factor of 1.33.

Figure (6) is a typical intensity pattern for an approximate plane wave of sound radiating through a slit of 18.2 mm width. The $\left(\frac{\sin\theta}{\theta}\right)^2$ appearance is distinct. For a slit of width L, the angle θ_0 between the first zeroes on either side of the central maximum is given by

$$\Delta\theta_o = \frac{4\pi}{KL} \qquad (3.2)$$

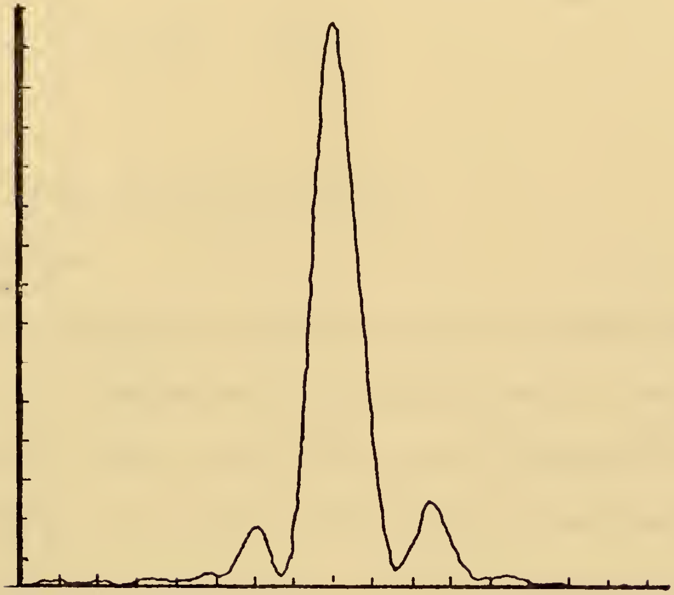

Figure (6) Angular spectrum of the intensity of the diffracted light due to a plane wave of sound radiating through an 18.2 mm slit

The apparent width of the sound field is changed by positioning a variable slit in front of the transducer. Viewed from the angular spectrum perspective, the construction of the slit can be very important. To be perfectly effective, the slit edges should be infinitely thin to avoid diffraction effects, the sides should be parallel, and its physical location centered on the angular spectrum of the source. For the system employed, these considerations were not optimized, and the resulting "edge effects" distorted the angular spectrum which was sampled such that the actual size of the slit employed is about .77 of the experimentally determined values. This factor is constant for all cases involving slits, however, and could be reduced with more consideration to the above factors.

That this intensity pattern actually does represent the sound field, however, can be shown through the similarity theorem [1] of the Fourier representation of the angular spectrum, which is that if

$$\mathcal{F}\{\underline{U}(x)\} = \underline{U}'(f_x) \tag{3.3}$$

then

$$\mathcal{F}\{a\underline{U}'(x)\} = \left|\frac{1}{a}\right| \underline{U}'\left(\frac{f_x}{a}\right) \tag{3.4}$$

where a is a constant.

The intensity patterns for vertical slits of several widths are shown in Fig. (7). Examination of the separation of the distance between the first zeroes on either side of the central maximum for each of the above cases reveals an expansion of the angular spectrum nearly equal to the factor by which the width of the slit was reduced (within 10%). Careful design of the slit would reduce this error. Because the amplitude of the central maximum decreased as the crossover points expanded, it was necessary to expand the amplitude scale for Fig. (7c) and Fig. (7d) in order to stay within the dynamic range of the x-y recorder. The crossover points were not affected by this change, however.

There are limitations on the narrowness of slit which may be employed due to a number of geometrical considerations. The width of the acoustic window frame and the distance from the source limit the angular spread of crossover points which can be transmitted into the area of light-sound interaction. Similarly, the width of the optical windows through which the laser beam passes constrains the angular rotation which can be measured. Both factors can be improved by design alterations of the present acoustic cell.

An interesting observation lies in examination of Fig. (8) which is the diffraction pattern due only to the width of the transducer. Because

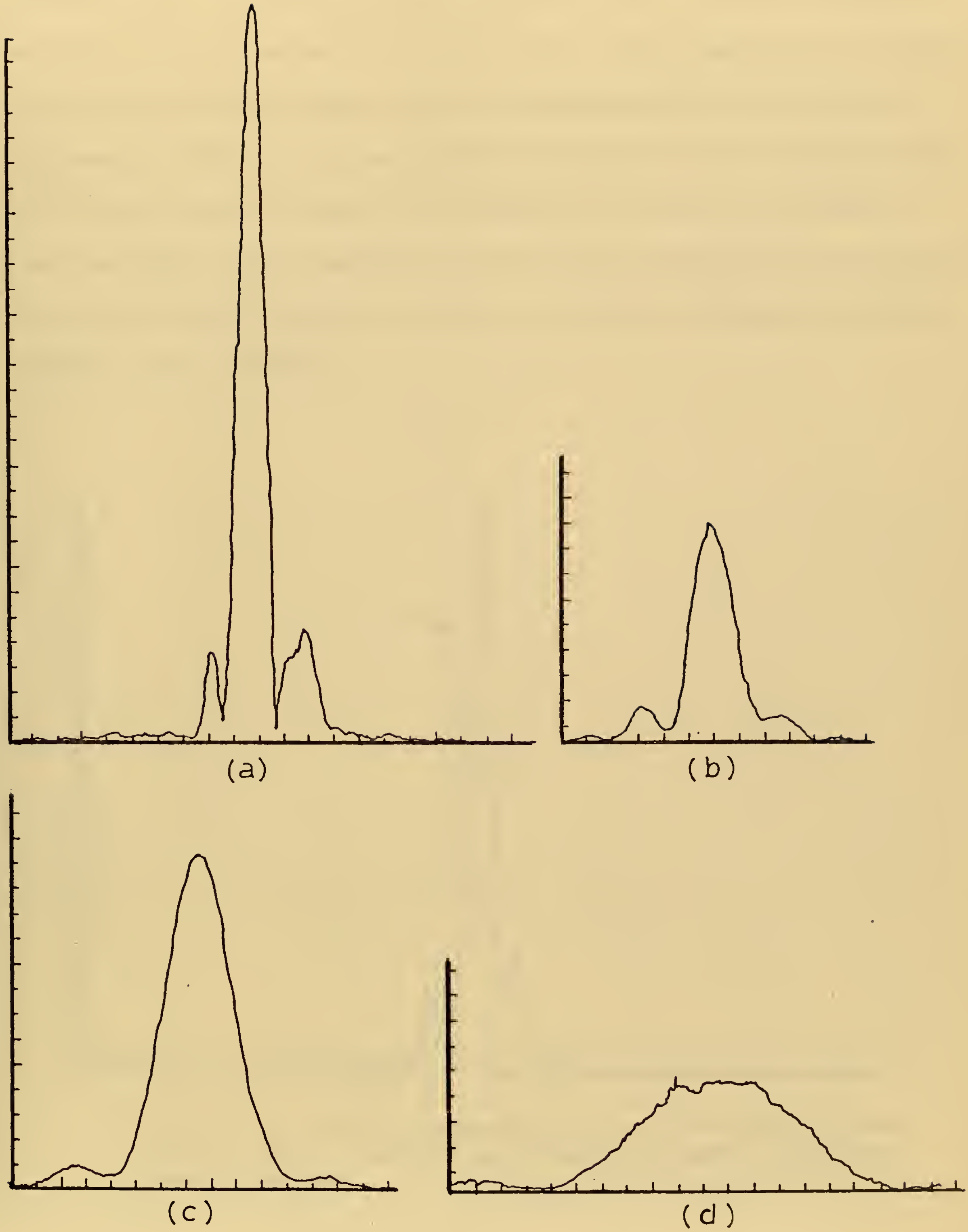

Figure (7) Angular intensity distribution of the diffracted light for slits in the sound fields of (a) 25.4, (b) 12.7, (c) 6.3, (d) 3.2 mm width. The separation between the first crossover points expands by the factor by which the slit is narrowed. (Note: Recorder sensitivity was changed between b and c.)

of the clamping at the edges, some difference in the geometry of the surface of equal amplitude sound is expected, i.e., a plane surface of amplitude will not extend to the full width of the transducer. The crossover corresponds to a plane surface of approximately 26 mm in width. Employment of slits of decreasing size to greater than 26 mm width yielded the same result; narrower slits exhibited the similarity property described above. This limitation of the width of the plane wave generated by this transducer has been verified by comparison with acoustic images obtained separately. [9]

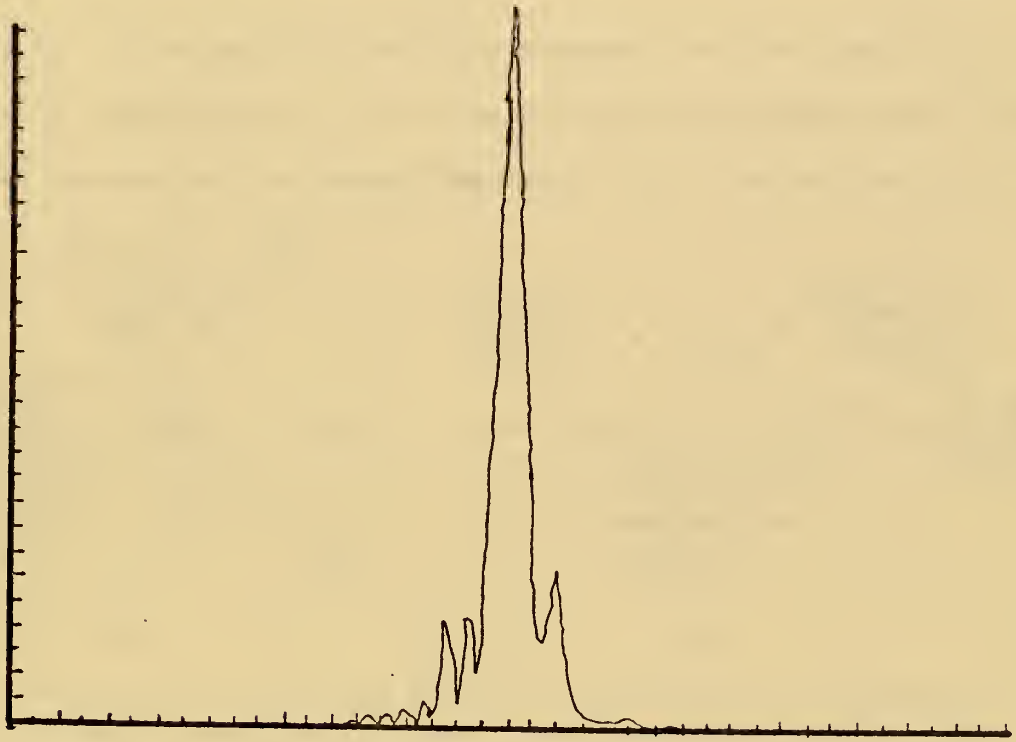

Figure (8) Diffraction pattern of the sound field without use of a slit. The 42.5 mm transducer appears to be only about 26 mm wide.

IV. APPLICATION

One application of the principle of Bragg diffraction probing lies in the examination of surface reflection and transmission phenomena. Consider, for example, sound in one fluid incident on the boundary of another fluid medium. The angle of reflection of the sound is equal to the angle of incidence, and the direction of the sound transmitted through the interface is governed by Snell's Law:

$$\frac{\sin \Theta_i}{c_1} = \frac{\sin \Theta_t}{c_2} \qquad (4.1)$$

where Θ_i is the angle of incidence measured from the normal, Θ_t is the angle of transmission, c_1 is the velocity of the incident sound, and c_2 is the velocity of the transmitted sound. Fig. (9a) depicts the situation.

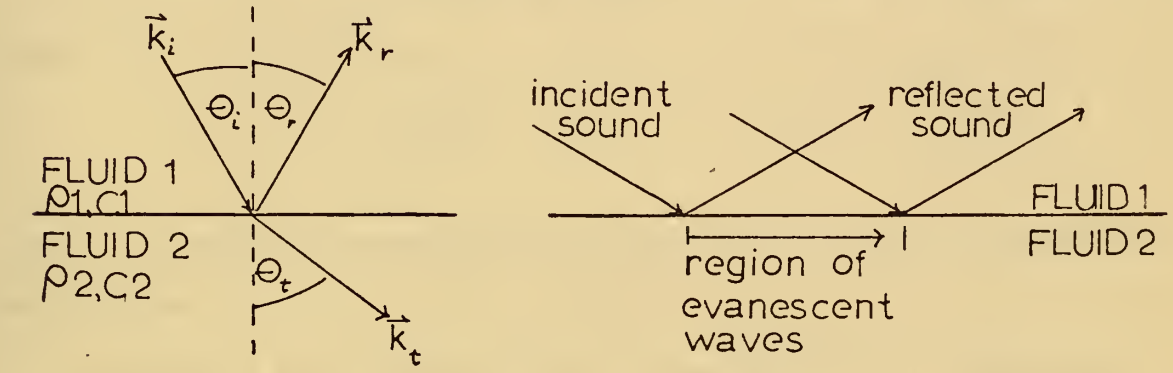

(a) (b)

Figure (9): (a) Sound incident on a fluid-fluid interface at an angle less than critical. In this instance $c_2 > c_1$, and the direction of transmission changes away from the normal. The vectors $\vec{k}_i$, $\vec{k}_r$, and $\vec{k}_t$ are the propagation vectors of the incident, reflected, and transmitted sound respectively. (b) Sound incident at a greater than critical angle. The region of evanescent waves is defined by the area insonified by the obliquely incident sound.

In the case where $c_2 > c_1$, there exists a critical angle, Θ_c given by

$$\Theta_c = \sin^{-1} \frac{c_1}{c_2} \qquad (4.2)$$

beyond which no energy is transmitted into the lower medium. [12] Instead, a wave creeping along the underside of the interface is generated in the area insonified by the obliquely incident sound as shown in Fig. (9b). Waves of this nature decay exponentially in depth and are known as "evanescent" waves. [13] The origin of these waves can be explained in the following manner.

A wave propagating in 3-dimensional space may be written

$$\underline{U}(x,y,z) = \underline{A}(x,y,z)e^{j(\vec{k}\cdot\vec{r} - \omega t)} \tag{4.3}$$

where $\underline{A}$ (x,y,z) is a complex-valued amplitude and phase function, and $\vec{k}$ is the propagation vector of the wave. The vector $\vec{r}$ is

$$\vec{r} = x\hat{x} + y\hat{y} + z\hat{z} \tag{4.4}$$

where $\hat{x}$, $\hat{y}$, and $\hat{z}$ are unit vectors along the x, y, and z axes respectively.

Completing the dot product, the propagating wave may be described by

$$\underline{U}(x\,y\,z) = \underline{A}(x\,y\,z)e^{j(k_x x + k_y y)}e^{jk_z z} \tag{4.5}$$

where

$$k_x = k\alpha \tag{4.6}$$

$$k_y = k\beta \tag{4.7}$$

$$k_z = k\gamma \tag{4.8}$$

(α, β, γ are again the direction cosines) and the time dependence has been dropped.

As stated in the preceding section, when $\alpha^2 + \beta^2 < 1$, wave propagation occurs in the normal manner as described above. When $\alpha^2 + \beta^2 > 1$, k_z becomes an imaginary number, $j|k_z|$ and the wave is described by

$$\underline{U}(x\,y\,z) = \underline{A}(x\,y\,z)e^{j(k_x x + k_y y)}e^{-|k_z|z} \tag{4.9}$$

where

$$|k_z| = \left|k\sqrt{1-\alpha^2-\beta^2}\right| \tag{4.10}$$

Thus, for the situation described, the wave travels in the x-y plane but attenuates exponentially in the z direction.

To see that the criterion above is actually met, consider a plane wave of sound of unit amplitude incident on a fluid-fluid boundary as in Fig. (9a). From Eq. (4.3) this is

$$\underline{U}_i(x,z) = e^{j(k_{1x}x + k_{1z}z)} \tag{4.11}$$

where the time and y dependence have been dropped for simplicity, and

$$k_1^2 = k_{1x}^2 + k_{1z}^2 \tag{4.12}$$

Since the angle of reflection equals the angle of incidence, the reflected wave can be written

$$\underline{U}_r(x,z) = \sqrt{a_r}\; e^{j(k_{1x}x - k_{1z}z)} \tag{4.13}$$

where a_r is the sound power reflection coefficient, given by [12]

$$a_r = \left(\frac{\rho_2 c_2 \mathrm{Cos}\,\theta_i - \rho_1 c_1 \mathrm{Cos}\,\theta_t}{\rho_2 c_2 \mathrm{Cos}\,\theta_i + \rho_1 c_1 \mathrm{Cos}\,\theta_t} \right)^2 \tag{4.14}$$

Since

$$k = \frac{\omega}{c} \tag{4.15}$$

Eq.(4.1) can be written

$$\frac{\mathrm{Sin}\,\theta_i}{\mathrm{Sin}\,\theta_t} = \frac{c_1}{c_2} = \frac{k_2}{k_1} \tag{4.16}$$

Then the transmitted ray can be written

$$\underline{U}_t(xz) = \sqrt{a_t}\; e^{j(k_{2x}x + k_{2z}z)} \tag{4.17}$$

where a_t is the sound power transmission coefficient given by

$$a_t = 1 - a_r \tag{4.18}$$

which can be considered to be an expression of conservation of acoustic energy at the interface, and

$$k_2^2 = k_{2x}^2 + k_{2z}^2 , \tag{4.19}$$

Let the angle of incidence reach the critical angle, given by Eq. (4.2). Then by substituting into Eq. (4.18), one sees that there is no sound power transmitted into medium 2, and all the acoustic energy is reflected. Since the amplitude of $\underline{U}_t(x,0) = 0$ the pressure at the interface is zero, and the amplitude of the reflected wave equals that of the incident wave.

Applying the geometrical situation to Eqs. (4.5) through (4.8), the conditions leading up to Eq. (4.9) now apply. Since there is no propagation in the z direction

$$\vec{k}_{z\,\text{incident}} + \vec{k}_{z\,\text{reflected}} = 0 \tag{4.20}$$

which is another way of saying that the normal components of the velocity equal zero (otherwise the interface would separate).

The geometrical situation is shown in Fig. (10), from which one can see that

$$\Lambda_2 = \frac{\Lambda_1}{\text{Sin}\,\theta} \tag{4.21}$$

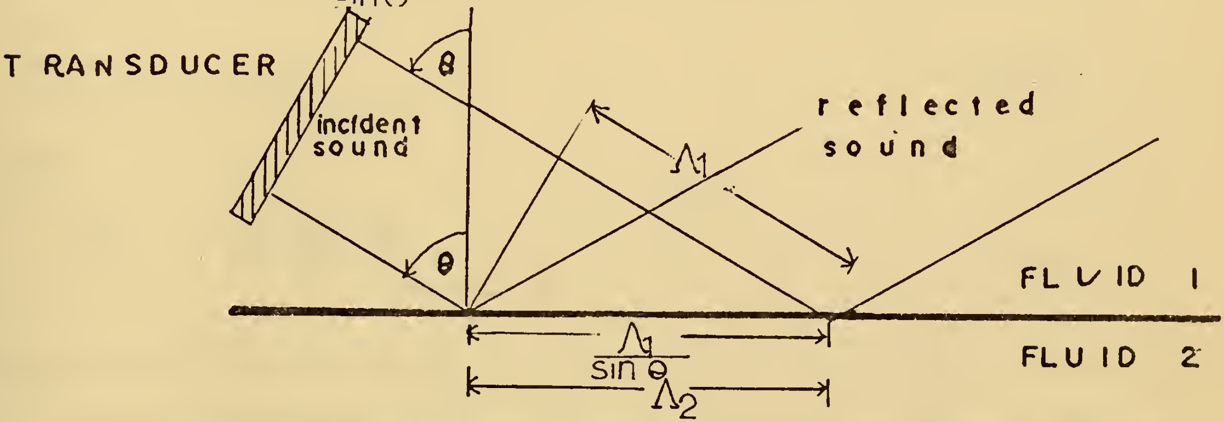

Figure (10) Geometrical considerations at an interface where evanescent waves are generated

Rearranging and multiplying by 2π

$$\frac{2\pi\,\text{Sin}\,\theta}{\Lambda_1} = \frac{2\pi}{\Lambda_2} = |k_{2x}| \tag{4.22}$$

Recalling Eq. (4.19) and substituting

$$\left(\frac{2\pi}{\Lambda_2}\right)^2 - \left(\frac{2\pi\,\text{Sin}\,\theta}{\Lambda_1}\right)^2 = k_{2z}^2 \tag{4.23}$$

factoring

$$\left(\frac{2\pi}{\Lambda_2}\right)^2 \left(1 - \frac{\Lambda_2 \text{Sin}\,\theta}{\Lambda_1}\right)^2 = k_{2z}^2 \tag{4.24}$$

but

$$\frac{\Lambda_2}{\Lambda_1} = \frac{c_2}{c_1} = \frac{1}{\text{Sin}\,\theta_c} \tag{4.25}$$

then

$$\left(\frac{2\pi}{\Lambda_2}\right)^2\left(1-\frac{\sin\theta}{\sin\theta_c}\right)^2 = k_{2z}^2 \tag{4.26}$$

Since θ is constrained such that

$$\theta > \theta_c \tag{4.27}$$

and

$$\frac{\sin\theta}{\sin\theta_c} > 1 \tag{4.28}$$

Thus k_{2z} is imaginary and

$$|k_{2z}| = |k_2 a_d| \tag{4.29}$$

where

$$a_d = \sqrt{1-\frac{\sin\theta}{\sin\theta_c}} \tag{4.30}$$

which agrees with Eq. (4.10)

From a physical point of view, since all of the energy was reflected there is a strong horizontal component (in the x direction) of velocity. If the amplitude of the transmitted sound were zero all the way to the interface, a discontinuity would occur, and the result would be shear waves at the boundary. Since liquids in general do not support shear, that infinitesimal thickness of medium 2 in contact with medium 1 takes the same velocity as medium 1. The wave in medium 2 is not driven, however, and so it decays with depth.

Evanescent waves in sound were first experimentally detected utilizing the principle of Bragg diffraction, by Wade, Powers, and deSouza [10], who used an acoustic grating to generate a propagating wave component in a direction normal to the grating, and a standing evanescent wave component located at and parallel to the back surface of the grating.

Illumination of the ultrasonic field under the Bragg condition yielded diffracted light components due to both sets of wave components, the evanescent portion being rotated 90 degrees about the undiffracted light from that of the normally propagated wave component.

For the configuration of Fig. (9), however, increasing the angle of incidence to the critical angle removes all waves except the evanescent waves. Illumination of the underside of the interface under the Bragg criteria, a method first proposed by Powers [11], results in a horizontally oriented spot of diffracted light which decays exponentially in amplitude as a function of depth.

Because the evanescent wave produced in this situation is a travelling wave [11], the frequency of the diffracted light is doppler-shifted as explained earlier, and demodulation of the diffracted light to obtain amplitude and phase information can be performed. This was not possible in the acoustic grating situation because the doppler shift from each of the oppositely directed evanescent waves that made up the standing wave cancelled out the frequency information contained in the diffracted light.

Exceeding the critical angle of incidence has another noticeable effect. Then

$$\Lambda_2 = \frac{\Lambda_1}{\sin\theta} \tag{4.31}$$

and as the angle of incidence is increased to beyond critical, Λ_2 decreases. As Λ_2 decreases, $\frac{\lambda}{2\Lambda}$ (the Bragg angle) becomes larger, and the diffracted light can be seen to move away from the undiffracted light.

Figure (11) shows the acoustic cell used in examination of the above theoretical predictions. A transducer similar to the one described earlier was mounted so as to provide an air backing, pinioned, and located above a turpentine-water interface. Because the density of turpentine

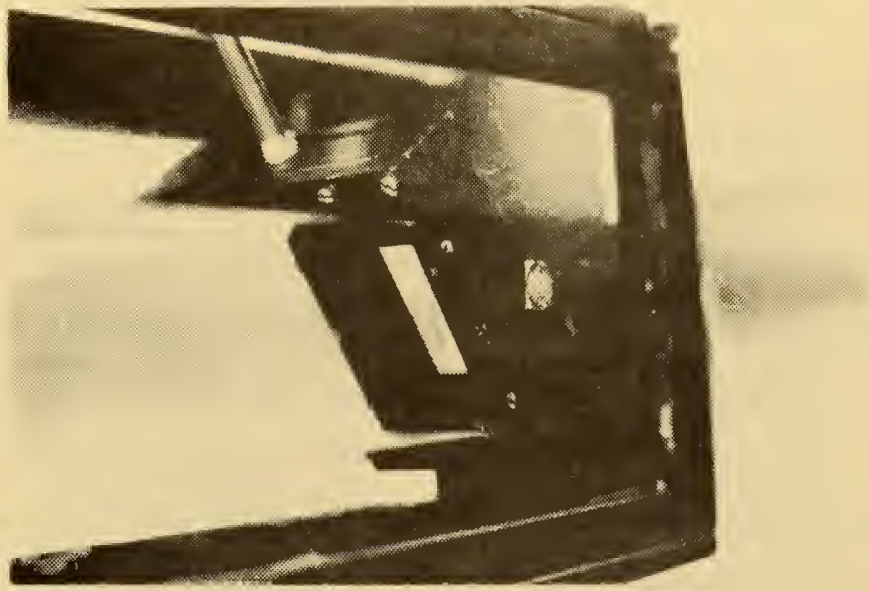

Figure (11) Acoustic cell used in interfacial reflection-transmission phenomena.

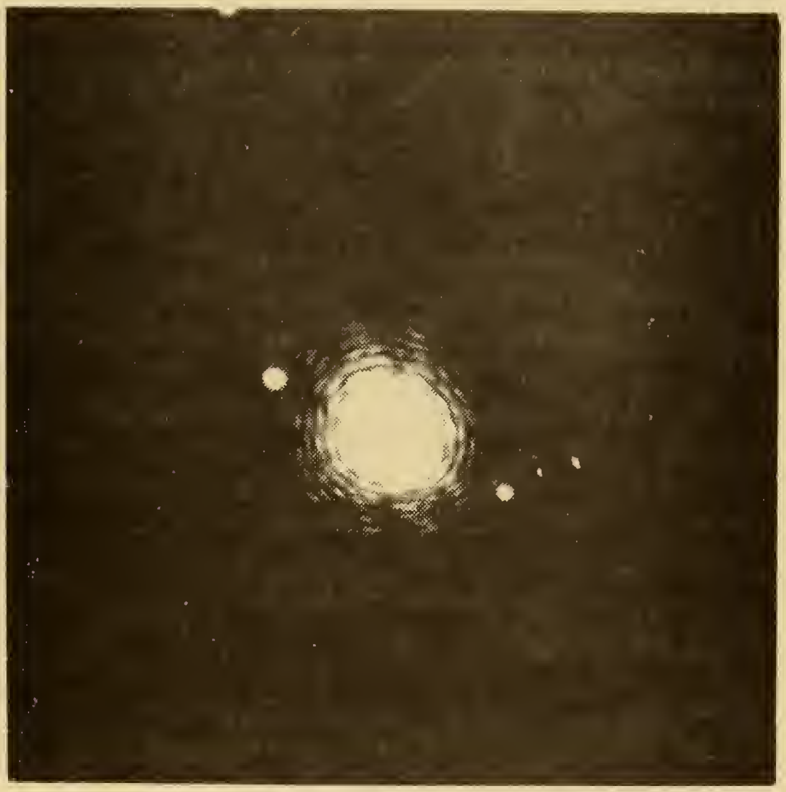

Figure (12) Diffracted up- and downshifted beams of light due to sound in turpentine incident on a water boundary.

ρ_1 = 870 Kg/m^3) is less than that of water (ρ_2 = 998 Kg/m^3), the turpentine overlaid the water, and the velocity of sound in turpentine is less than that of water (c_1 = 1250 m/sec, c_2 = 1481 m/sec). From the definition of θ_c, the critical angle was 57.6°.

Light from a helium-neon laser (λ = 6328 Å) was passed through a pinhole to illuminate the sound field at the Bragg angle to produce diffracted light in the manner described earlier. The light entered the acoustic cell from the opposite side pictured.

Figure (12) is a result of the Bragg interaction with the obliquely incident plane wave of sound. The direction of propagation is from the upper left to the lower right. The angle of the light with respect to the sound was such as to enhance the downshifted beam of diffracted light (the upper left spot). The circular concentric rings (known as an Airy Disc) about the undiffracted light are due to diffraction of the laser beam at the pinhole prior to entering the turpentine.

Figure (13) shows the same situation with the angle of incident light slightly altered to interact with the reflected wave. The lower right spot is the same as in the previous figure, representing the upshifted version of the incident sound while the lower left spot is that of the upshifted reflected sound.

Moving the incident light through the interface into the water, one can see in Fig. (14) the diffracted light from the sound transmitted through the interface when the angle of incidence is well less than the critical angle. The decrease in intensity of the transmitted sound is clearly noticeable. Figure (15) shows the downshifted diffracted ray of the transmitted sound when the angle of incidence has been increased by approximately 8°, but is still below the critical angle. Comparison

of the two figures demonstrates the counter-clockwise rotation of the diffracted light as the angle of incidence is increased.

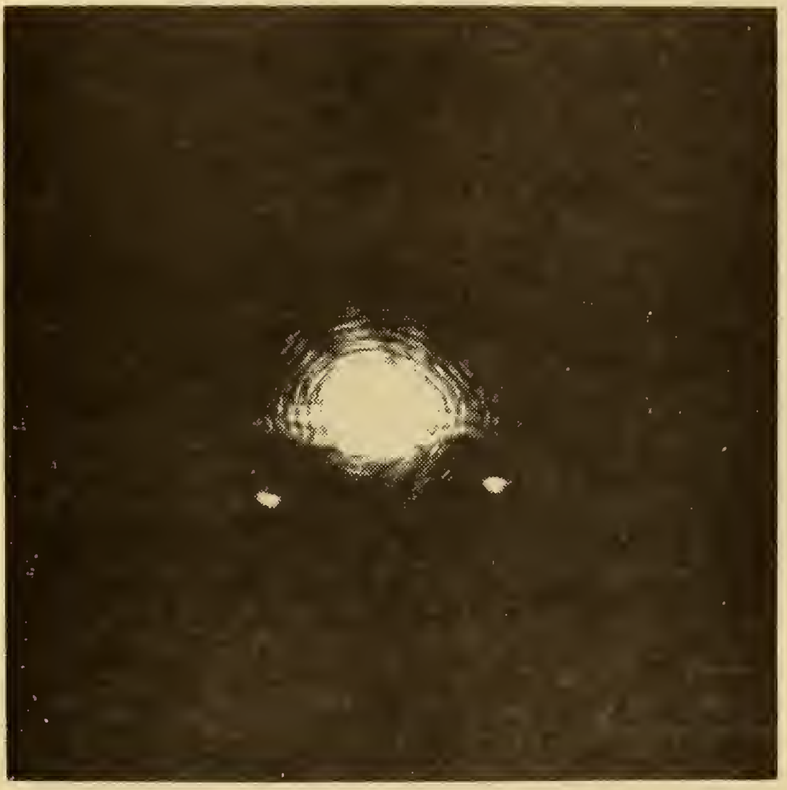

Figure (13) Upshifted diffracted light due to incident and reflected sound at a turpentine-water interface.

Figure (14) Diffracted light due to transmitted sound below the interface at an angle less than critical.

Figure (15) Diffracted light due to sound transmitted below the interface at an increased angle less than critical.

Figure (16) shows the diffracted light at an angle slightly greater than critical, and its horizontal position with respect to the undiffracted light indicates the plane of propagation of the evanescent waves. Increasing the angle of incidence by about one degree, one detects a slight outward horizontal shift of the diffracted light from the evanescent waves as expected. Comparison of Fig. (16) with Fig. (17) shows a shift of approximately half the distance between the neighboring rings on the Airy Disc illustrating this effect.

Figure (18) is a plot of the diffracted light intensity versus depth, and the exponentially decaying behavior is apparent. The experimentally determined decay rate of $1.6 \times 10^{-3}m^{-1}$ compares to an expected $1.1 \times 10^{-3}m^{-1}$.

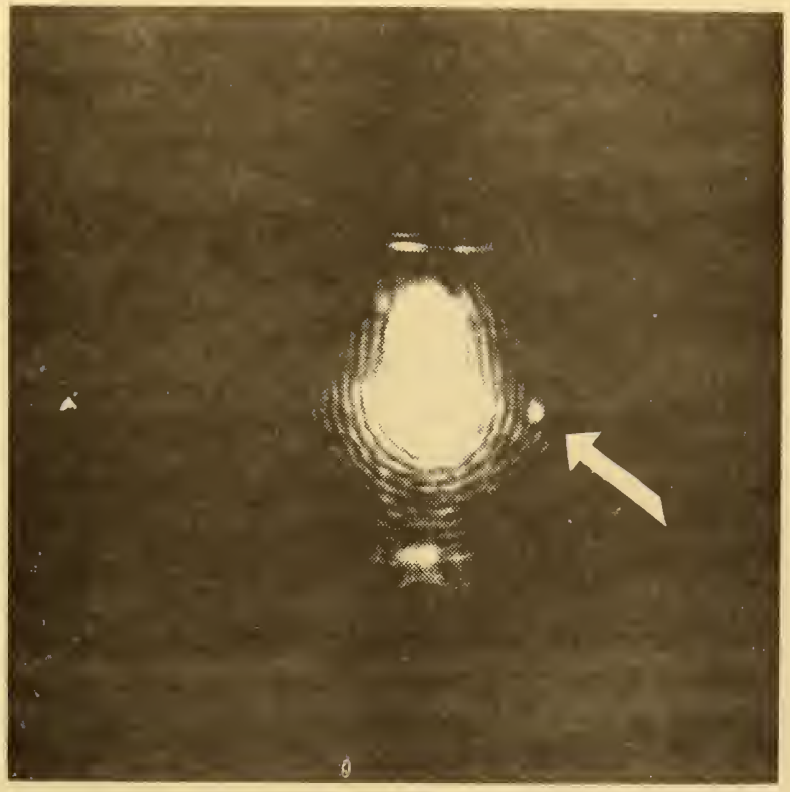

Figure (16) Diffracted light due to an evanescent wave when the angle of incidence is slightly greater than critical.

Figure (17) Diffracted light due to an evanescent wave when the angle of incidence is greater than in Fig. (15). The outward shift of the diffracted light is apparent.

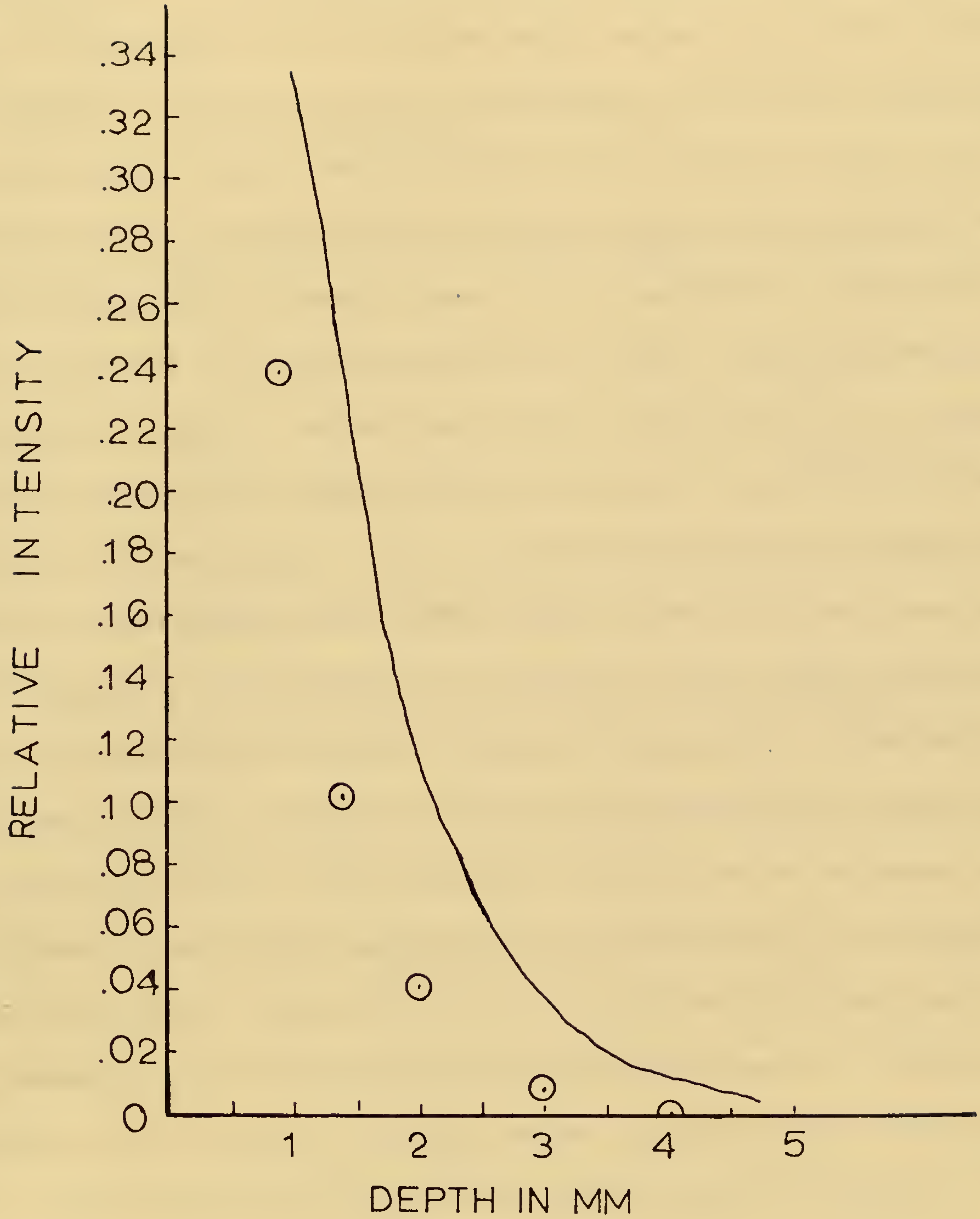

Figure (18) Plot of intensity of an evanescent wave versus depth.

V. CONCLUSION

Probing with a thin laser beam in a near ultrasonic field at a frequency of 15 megahertz in a distilled water medium has yielded a diffracted beam of light containing a Fourier relationship to the near field description of the sound field. The amplitude of the diffracted light, as a function of the angle between the incident light and the direction of acoustic propagation, is proportional to the amplitude of the spatial Fourier transform of the ultrasonic distribution. This verifies the principle and technique established by Cohen and Gorden [3] at frequencies of 50-250 megahertz in a quartz medium and provided experimental familiarity with the technique. Indication that this method of probing may be useful in evaluating transducer mounting schemes has been presented.

The intensity of the diffracted light due to the sound transmitted through a liquid-liquid interface decreased noticeably. Quantitative measurement of this intensity with the technique described combined with the geometry for which it was obtained is sufficient to determine density, index of refraction, and absorption coefficient of the transmission.

The principle of Bragg Diffraction of light has also been used to experimentally detect the presence of evanescent waves at a liquid-liquid interface when the angle of incident sound was greater than the critical angle, and to measure the properties of these evanescent waves.

BIBLIOGRAPHY

1. Goodman, J. W., Introduction to Fourier Optics, pp 7-9, 21-25, 48-51, McGraw-Hill, 1968.

2. Korpel, A., Kessler, L. W., and Ahmed, M., "Bragg Diffraction Sampling of a Sound Field," Journal of the Acoustical Society of America, Vol. 51, No. 5 (part 2) pp 1582-1591

3. Cohen, M. G. and Gordon, E. I., "Acoustical Beam Probing Using Optical Techniques," Bell System Technical Journal, Vol. XLIV, No. 4, April 1965.

4. Slater, J. C. "Interaction of Waves in Crystals," Reviews of Modern Physics, Vol. 30, No. 1, pp 197-198, January 1958.

5. Adler, R., "Interaction Between Light and Sound," IEEE Spectrum, Vol. 4, pp 44-48, May 1967.

6. Quate, C. F., Wilkinson, C. D., and Winslow, D. K., "Interaction of Light and Microwave Sound," Proceedings of the IEEE, Vol. 53, No. 10, pp 1604-1612, October 1965.

7. Powers, J. P., "Spatial Filtering Considerations in Bragg Diffraction Imaging," Acoustical Holography, Vol. 4, Plenum Publishing Corporation, 1972.

8. Korpel, A., The Interaction of Sound and Light Fields of Arbitrarily Prescribed Cross-Section, Zenith Radio Corporation Research Report No. 66-2, September 1966.

9. Powers, J. P., Private Communication

10. Wade, G., Powers, J. P., deSouza, A. A., "Experimental Detection of Evanescent Ultrasonic Waves by Bragg Diffraction of Light," Journal of the Acoustical Society of America, Vol. 45, pp 1247-1250, 1969.

11. Powers, J. P., Some Aspects of the Application of Bragg Diffraction of Laser Light to the Imaging and Probing of Acoustic Fields, Ph. D. Thesis, University of California, Santa Barbara, 1970.

12. Kinsler, L. E. and Frey, A. R., Fundamentals of Acoustics, 2d ed., pp 128-150, John Wiley and Sons, Inc., 1962.

13. Fowles, G. R., Introduction to Modern Optics, pp 50-56, Holt, Rinehart, and Winston Inc., 1968.

INITIAL DISTRIBUTION LIST

		No. Copies
1.	Defense Documentation Center Cameron Station Alexandria, Virginia 22314	2
2.	Library, Code 0212 Naval Postgraduate School Monterey, California 93940	2
3.	Asst. Professor J. P. Powers, Code 52 Po Department of Electrical Engineering Naval Postgraduate School Monterey, California 93940	1
4.	Lt. Robert D. Brown, Jr. USS Purdy (DD 734) %Fleet Post Office New York, New York 09501	1

Unclassified
Security Classification

DOCUMENT CONTROL DATA - R & D

(Security classification of title, body of abstract and indexing annotation must be entered when the overall report is classified)

1. ORIGINATING ACTIVITY *(Corporate author)* Naval Postgraduate School Monterey, California 93940	2a. REPORT SECURITY CLASSIFICATION Unclassified 2b. GROUP

3. REPORT TITLE
An Investigation of the Principles and Techniques of Bragg Diffraction Laser Beam Probing of an Ultrasonic Field

4. DESCRIPTIVE NOTES *(Type of report and, inclusive dates)*
Master's Thesis (December 1972)

5. AUTHOR(S) *(First name, middle initial, last name)*
Robert David Brown, Jr.

6. REPORT DATE	7a. TOTAL NO. OF PAGES	7b. NO. OF REFS
December 1972	38	13

8a. CONTRACT OR GRANT NO. b. PROJECT NO. c. d.	9a. ORIGINATOR'S REPORT NUMBER(S) 9b. OTHER REPORT NO(S) *(Any other numbers that may be assigned this report)*

10. DISTRIBUTION STATEMENT
Approved for public release; distribution unlimited.

11. SUPPLEMENTARY NOTES	12. SPONSORING MILITARY ACTIVITY
	Naval Postgraduate School Monterey, California 93940

13. ABSTRACT

Probing of the near field of an ultrasonic beam in water with a thin laser beam has verified that a diffracted beam of light, whose amplitude is a function of the angle of incident light, is related to the spatial Fourier spectrum of the far-field acoustic distribution. There are indications that this method of probing may be useful in evaluating transducer mountings.

As an application of the technique, reflection-transmission properties of sound on a liquid-liquid interface are examined, and the detection of evanescent waves verifies their physical existence and properties.

DD FORM 1 NOV 65 1473 (PAGE 1)
/N 0101-807-6811

Unclassified
Security Classification

A-31408

Unclassified

Security Classification

14. KEY WORDS	LINK A		LINK B		LINK C	
	ROLE	WT	ROLE	WT	ROLE	WT
1. Light-Sound Interaction						
2. Bragg Diffraction						
3. Laser Beam Ultrasonic Probing						
4. Critical Angle of Incidence						
5. Evanescent Waves						

Thesis
B8223
c.1

141218

Brown

An investigation of the principles and techniques of Bragg diffraction laser beam probing of an ultrasonic field.